

NASA TECHNICAL NOTE



NASA TN D-5493

C. 1



NASA TN D-5493

LOAN COPY: RETURN TO
AFWL (W10L-2)
KIRTLAND AFB, N MEX

DISLOCATION STRUCTURES IN SINGLE CRYSTAL TUNGSTEN AND TUNGSTEN ALLOYS

by Joseph R. Stephens
Lewis Research Center
Cleveland, Ohio

NATIONAL AERONAUTICS AND SPACE ADMINISTRATION • WASHINGTON, D. C. • OCTOBER 1969



0132142

1. Report No. NASA TN D-5493	2. Government Accession No.	3. Recipient's Catalog No.
4. Title and Subtitle DISLOCATION STRUCTURES IN SINGLE CRYSTAL TUNGSTEN AND TUNGSTEN ALLOYS		5. Report Date October 1969
7. Author(s) Joseph R. Stephens		6. Performing Organization Code
9. Performing Organization Name and Address Lewis Research Center National Aeronautics and Space Administration Cleveland, Ohio 44135		8. Performing Organization Report No. E-5098
12. Sponsoring Agency Name and Address National Aeronautics and Space Administration Washington, D.C. 20546		10. Work Unit No. 129-03
15. Supplementary Notes		11. Contract or Grant No.
16. Abstract Deformation of tungsten single crystals as a function of strain, temperature, and alloying was studied by transmission electron microscopy. Unalloyed tungsten, W-1 and 3 percent Re, and W-1 and 3 percent Ta single crystals oriented for $(\bar{1}01)$ $[111]$ slip were deformed in compression at 150, 300, and 590 K. Transmission microscopy revealed that the substructure in unalloyed tungsten is similar to substructures in other refractory metals when compared on the basis of homologous temperature. The primary effect of rhenium additions is to produce edge dipoles in the wake of screw dislocations. Tantalum had a lesser effect on dislocation substructure.		13. Type of Report and Period Covered Technical Note
17. Key Words (Suggested by Author(s)) Dislocations Single crystal tungsten	18. Distribution Statement Unclassified - unlimited	14. Sponsoring Agency Code
19. Security Classif. (of this report) Unclassified	20. Security Classif. (of this page) Unclassified	21. No. of Pages 22
		22. Price* \$3.00

*For sale by the Clearinghouse for Federal Scientific and Technical Information
Springfield, Virginia 22151

DISLOCATION STRUCTURES IN SINGLE CRYSTAL TUNGSTEN AND TUNGSTEN ALLOYS

by Joseph R. Stephens

Lewis Research Center

SUMMARY

Deformation of tungsten single crystals as a function of strain, temperature, and alloying was studied by transmission electron microscopy. Single crystals oriented for $(\bar{1}01)$ $[111]$ slip were grown by electron beam zone refining. Compression specimens of tungsten (W), tungsten - 1 percent rhenium (W-1Re), tungsten - 1 percent tantalum (W-1Ta), and tungsten - 3 percent tantalum (W-3Ta) were deformed to 2 percent strain at 150, 300, and 590 K (0.04, 0.08, and 0.16 homologous temperature, T_m (fraction of absolute melting temperature)). Specimens were also strained to 0.5 and 5.0 percent strain at 300 K.

Transmission microscopy revealed that the dislocation substructures in single crystal tungsten are similar to substructures in other refractory metals when compared on the basis of homologous temperature. At temperatures greater than $0.1 T_m$, the substructure is characterized primarily by edge dipoles. At temperatures less than $0.1 T_m$, long screw dislocations lying parallel to the primary $[111]$ slip direction characterize the substructure. Rhenium additions to tungsten promote formation of edge dipoles at temperatures of 150 and 300 K and increase dislocation density at all three temperatures. In addition, dislocations consistent with $(\bar{1}\bar{1}2)$ $[\bar{1}11]$ slip were observed in the W-Re single crystals after deformation at 150 K. Tantalum additions had a lesser effect on the dislocation substructure compared with rhenium additions. The W-1Ta and W-3Ta alloys exhibited higher dislocation densities than unalloyed tungsten after similar strains and, at 150 K, W-3Ta contained a few dislocations consistent with $(\bar{1}\bar{1}2)$ $[\bar{1}11]$ slip.

It is concluded that the reduction in ductile-brittle transition temperature of polycrystalline tungsten containing dilute rhenium additions, 1 to 5 percent, can be attributed to an increase in dislocation mobility at temperatures less than $0.1 T_m$.



INTRODUCTION

Deformation behavior of the refractory metals has been the subject of a number of investigations over the past decade. Dislocation arrangements have been studied by the technique of transmission electron microscopy, most frequently in polycrystalline metals deformed by rolling followed by annealing in the recovery and recrystallization temperature range. Low temperature deformation (temperature less than $0.2 T_m$) in tension or compression has also been studied in polycrystalline refractory metals and alloys by transmission electron microscopy, for example, niobium by Harris (ref. 1), tantalum by Barbee and Huggins (ref. 2), molybdenum by Gilbert, Wilcox, and Hahn (ref. 3), and tungsten by Stephens (ref. 4).

To obtain a clearer understanding of the mechanisms controlling the deformation of the refractory metals, interest has shifted to more detailed, quantitative transmission electron microscopy studies on preoriented single crystal specimens with foils sectioned parallel to operative slip planes. The effects of temperature and strain on dislocation structures have been studied in niobium by Foxall, Duesbery, and Hirsch (ref. 5) and and Bowen, Christian, and Taylor (ref. 6), in tantalum by Spitzig and Mitchell (ref. 7), and Aresnault and Lawley (ref. 8), and in molybdenum by Loesch and Brotzen (ref. 9) and Lawley and Gaigher (refs. 10 and 11). Deformation mechanisms in single crystal tungsten have not previously been studied in detail by transmission electron microscopy.

Because of the interest in tungsten as a structural material and the desirability of understanding the deformation behavior of tungsten and tungsten alloys near room temperature, the present investigation was conducted to characterize the dislocation substructure of single crystal tungsten as a function of strain, temperature, and dilute alloy additions. Specimens oriented for $(\bar{1}01)$ $[111]$ slip were deformed in compression to a maximum strain of 5.0 percent. Test temperatures were 150, 300, and 590 K, or 0.04 , 0.08 , and $0.16 T_m$, respectively. Alloy additions included 1 and 3 percent rhenium and 1 and 3 percent tantalum. Both alloy additions have been shown to be effective in reducing the ductile-brittle transition temperature of polycrystalline tungsten. Rhenium additions induce a strong solution softening effect in tungsten at temperatures less than $0.1 T_m$ (ref. 12), a phenomenon observed in many body centered cubic dilute solid solutions.

Observations on tungsten foils cut parallel to the $(\bar{1}01)$ slip plane are compared with dislocation structures observed by other investigators in other refractory metals tested under similar conditions. Effects of dilute rhenium and tantalum additions on dislocation structures in tungsten and the implications of the results on the ductile-brittle transition temperature and solution softening in polycrystalline specimens are discussed.

EXPERIMENTAL PROCEDURE

Materials

Two-pass electron-beam zone-refined rods of tungsten, W-1Re, W-3Re, W-1Ta, and W-3Ta were used for this investigation. The first zoning pass melted and purified the sintered and swaged rods, while seeding to the desired orientation was accomplished during the second pass. Chemical analyses of the crystals are given in table I. Single crystals were oriented for single slip on the $(\bar{1}01)$ $[111]$ slip system (fig. 1). Orientations of the single crystals fell within the shaded area shown in figure 1, and the Schmid factor ranged from 0.494 to 0.499 on the $(\bar{1}01)$ slip plane.

TABLE I. - CHEMICAL ANALYSES OF ZONE-REFINED RODS

Rod composition (nominal)	Rod composition (analyzed)					
	wt. %			ppm		
	W	Re	Ta	C	O	N
W	Balance	----	----	<2	4	0.6
W - 1 Re	↓	0.85	----	↓	3	.5
W - 3 Re		3.0	----		3	<.5
W - 1 Ta		----	0.87		2	<.5
W - 3 Ta	↓	----	3.0	↓	1	<.5

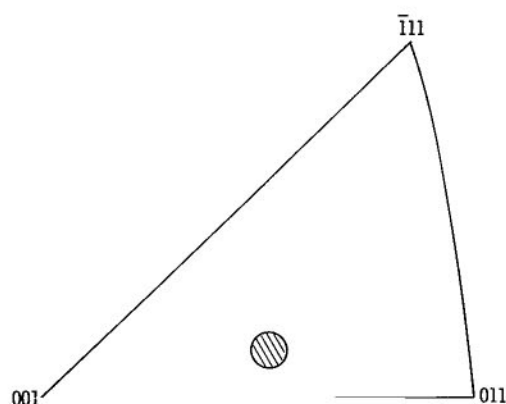


Figure 1. - Unit triangle showing orientation of single crystals, shaded area, used in this investigation for $(\bar{1}01)$ $[111]$ slip.

Compression Tests

Compression specimens 7.6 millimeters long by 3.3 millimeters in diameter were ground from the zone melted single crystals and subsequently electropolished in a 2.0 percent sodium hydroxide solution to a diameter of 3.2 millimeters to remove surface defects resulting from grinding. Compression tests were conducted in a hard universal testing machine at a strain rate of 0.055 percent per second. Specimens were compressed to a strain of 2.0 percent at 150, 300, and 590 K, or 0.04, 0.08, and 0.16 T_m , respectively. Specimens were also compressed to strains of 0.5 and 5.0 percent at 300 K. Strain was recorded autographically from crosshead movement, and load was recorded from a strain gage load cell.

Thin Foil Preparation

Disks approximately 0.3 millimeter thick were cut from the deformed specimens parallel to the $(\bar{1}01)$ primary slip plane by electrical discharge machining. The primary $[111]$ slip direction lies nearly parallel to the major axis of the elliptical shaped disks that were cut parallel to the $(\bar{1}01)$ plane. This direction was scribed on the disk and used as a reference during subsequent examination in the electron microscope and analysis of electron diffraction patterns so that Burgers vectors could be determined unambiguously. Disks were thinned electrolytically in a 1.0 percent sodium hydroxide solution at a temperature of approximately 280 K. A combination specimen holder and thinning apparatus designed by Schoone and Fishione (ref. 13) which permits jet and bath polishing simultaneously was used for thinning purposes. Foils were examined in a JEM 7A electron microscope operated at 100 kilovolts. Identification of Burgers vectors was accomplished by contrast experiments using a tilting-rotating stage.

Measurements of Dislocation Density

A method in general use for dislocation density measurements is to count the number of intersections with dislocations made by random lines drawn on micrographs. This method has the disadvantage of being affected by nonrandom distribution of dislocations leading to low values of dislocation density ρ (ref. 14). One method of overcoming the effect of an anisotropic dislocation distribution in the plane of the foil is to count intersections of dislocations with a series of circles. Dislocation density is then given by

$$\rho = \frac{2n}{Lt}$$

where

ρ dislocation density, cm^{-2}

n number of intersections which dislocations make with a series of six randomly spaced circles of uniform diameter

L total circumference of the six circles, 40 cm

t foil thickness (a value of 2000 Å used for the calculations)

RESULTS

Stress-Strain Behavior

Stress-strain curves for single crystal tungsten and tungsten alloys are shown in figure 2. Moderate work hardening increasing with decreasing temperature occurs for single crystal tungsten and tungsten alloys oriented as shown in figure 1. Similar stress-strain behavior has been observed by Garlick and Probst (ref. 15) on single crystal tungsten oriented for $(\bar{1}01)$ slip and by Garfinkle (ref. 16) on single crystal tungsten and a W-3.0Re alloy oriented for $(1\bar{1}2)$ slip. In contrast, tungsten oriented for $(\bar{2}11)$ slip (ref. 15) and W-5.0Re to W-9.0Re alloys oriented for $(1\bar{1}2)$ slip (ref. 16) exhibit essentially no work hardening after yielding.

Figure 3 shows the effect of alloying on the 2.0 percent flow stress at the three temperatures investigated in this study. Solution softening is observed for both alloy additions at each temperature. The minimum in flow stress at a concentration of 1.0 Re at 150 K is unexpected since solution softening at this temperature in polycrystalline W-Re alloys extends over a much larger range of rhenium content as shown by Raffo (ref. 17).

Transmission Microscopy

The strain dependence of dislocation substructures for single crystal tungsten and tungsten alloys oriented for $(\bar{1}01)$ $[111]$ slip is shown in figures 4 to 6. Foils were cut parallel to the $(\bar{1}01)$ slip plane after various deformations in compression at room temperature (300 K). For ease of comparison, all micrographs in figure 4 and subsequent figures are oriented with the primary $[111]$ slip direction pointing to the top of the page. A minimum of twelve micrographs was taken of regions throughout each foil. The following paragraphs describe the observations that were made and the accompanying figures serve to illustrate the observations.

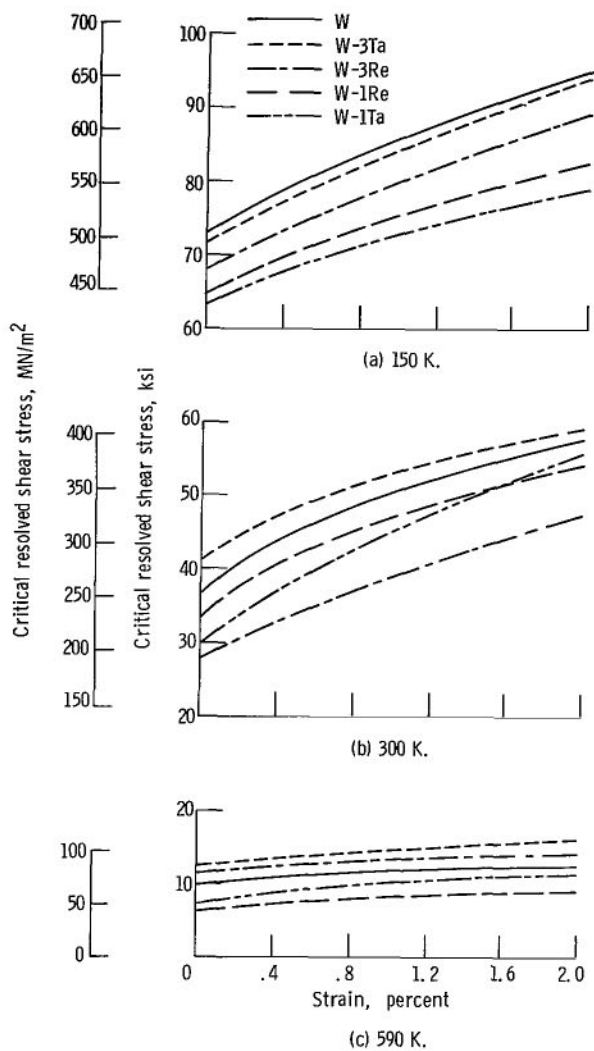


Figure 2. - Stress-strain curves for W and W alloy single crystals at various temperatures.

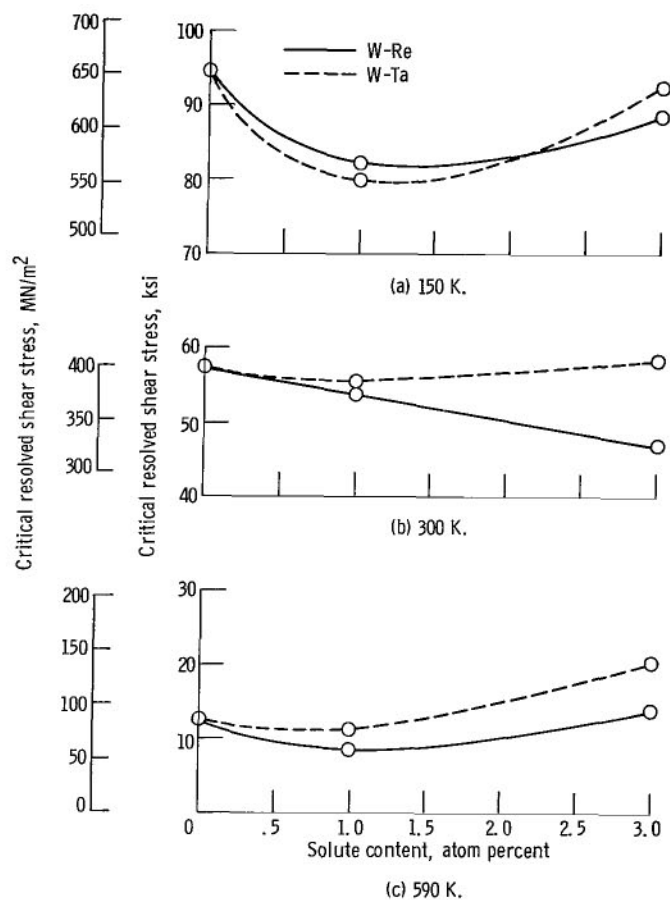


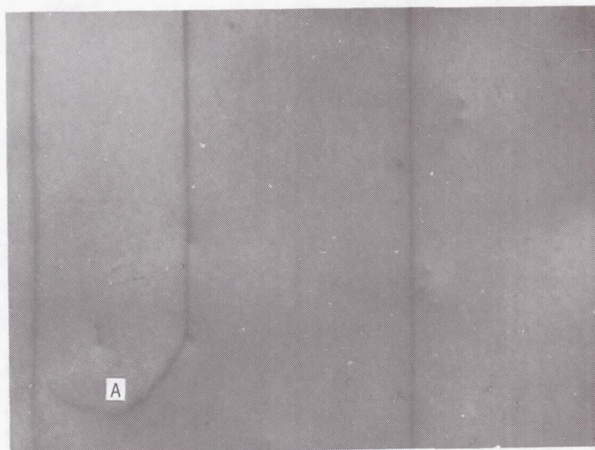
Figure 3. - Effect of solute concentration on 2-percent flow stress for W-Re and W-Ta alloy crystals deformed in compression at various temperatures.



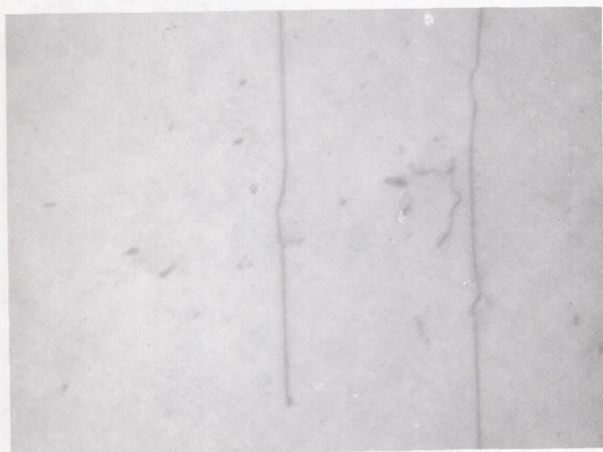
(a) Unalloyed tungsten.



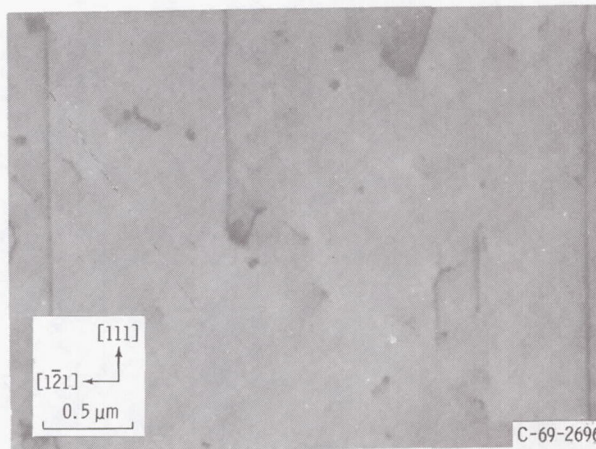
(b) W - 1 percent Re.



(c) W - 3 percent Re.



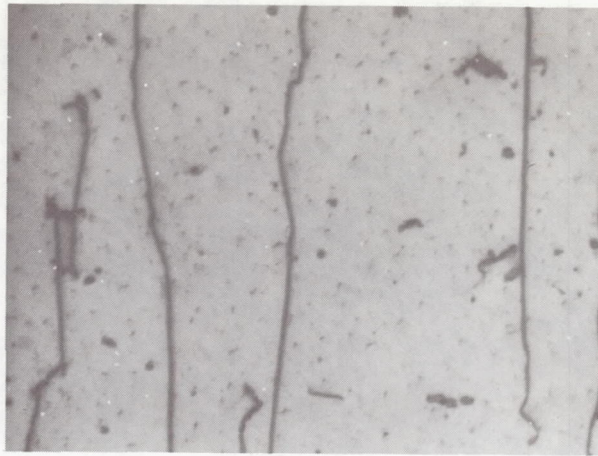
(d) W - 1 percent Ta.



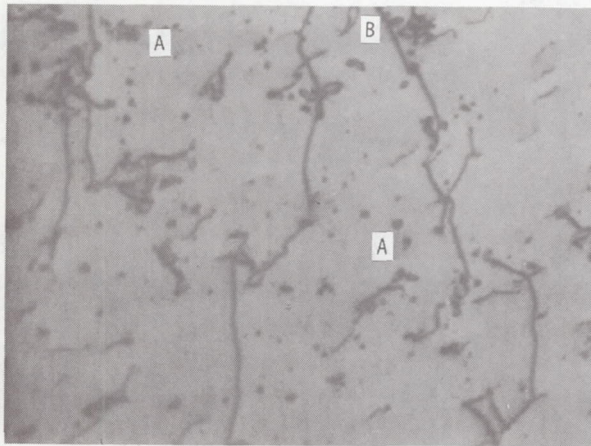
(e) W - 3 percent Ta.

C-69-2696

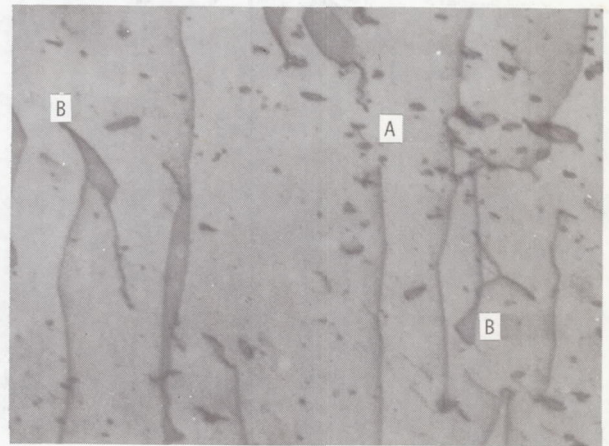
Figure 4. - Dislocation structures after 0.5 percent strain at 300 K.



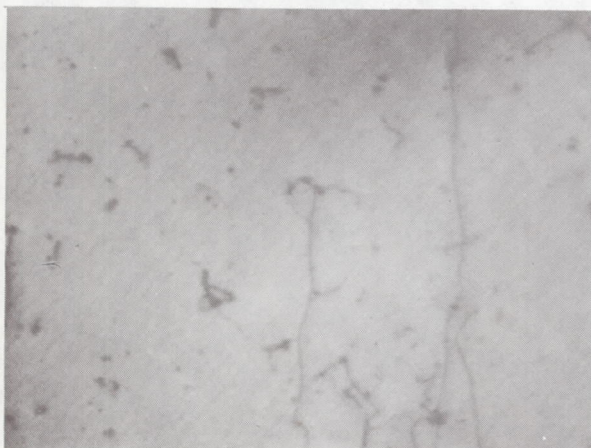
(a) Unalloyed tungsten.



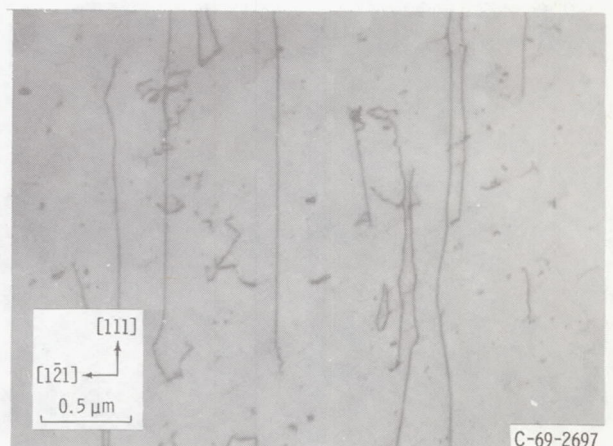
(b) W - 1 percent Re.



(c) W - 3 percent Re.

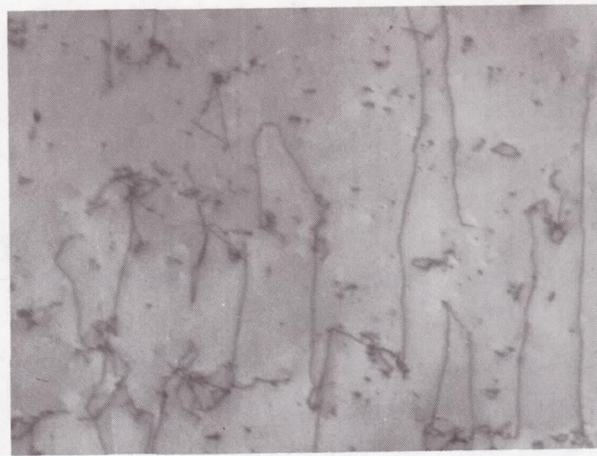


(d) W - 1 percent Ta.

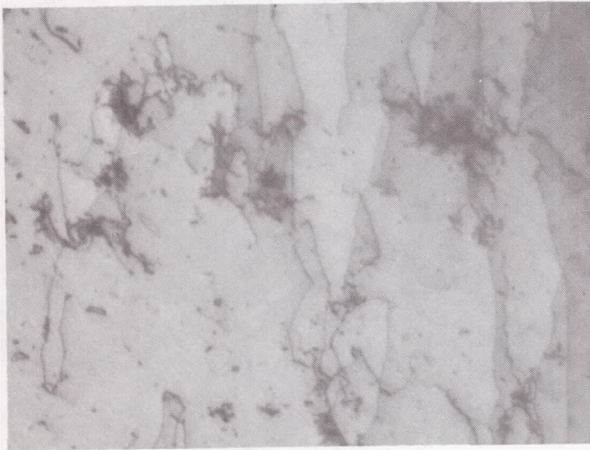


(e) W - 3 percent Ta.

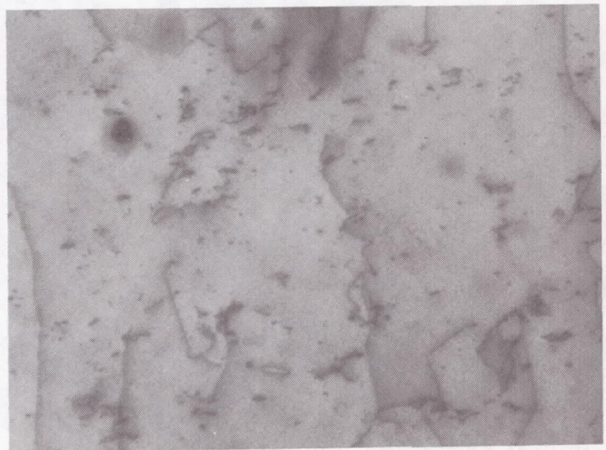
Figure 5. - Dislocation structures after 2.0 percent strain at 300 K.



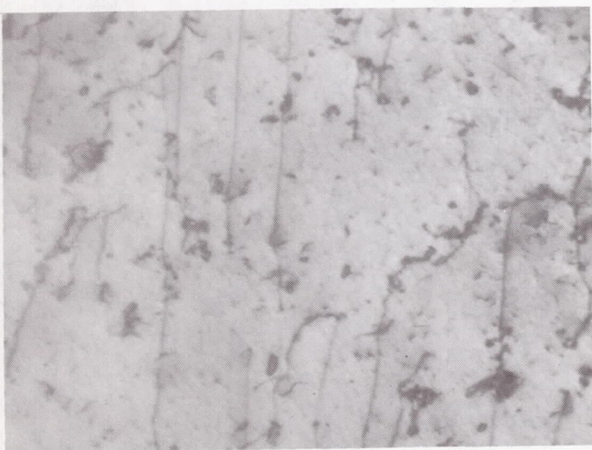
(a) Unalloyed tungsten.



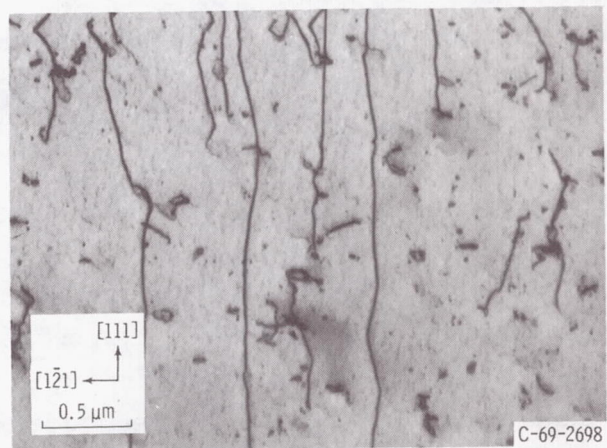
(b) W - 1 percent Re.



(c) W - 3 percent Re.



(d) W - 1 percent Ta.



(e) W - 3 percent Ta.

Figure 6. - Dislocation structures after 5.0 percent strain at 300 K.

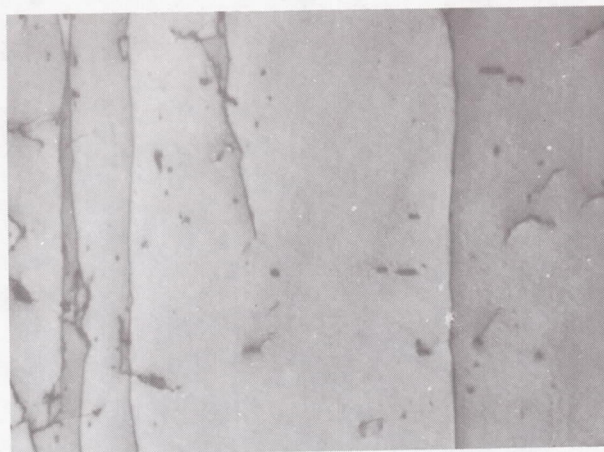
The substructures are characterized by long screw dislocations lying parallel to the primary [111] slip direction after a strain of 0.5 percent, as shown in figure 4. Frequent jogs are noted on the screw dislocations in unalloyed tungsten, W-1Re, W-1Ta, and W-3Ta alloys. The W-3Re alloy is characterized by nearly straight dislocations except for occasional mixed dislocations as at A in figure 4(c).

After a strain of 2.0 percent, the dislocations have the same general characteristics in unalloyed tungsten and the W-Ta alloys as observed after 0.5 percent strain. In the W-Re alloys, a relatively high density of debris or small loops formed as noted at A in figures 5(b) and (c). Formation of these or edge dipoles can be seen at B in these figures.

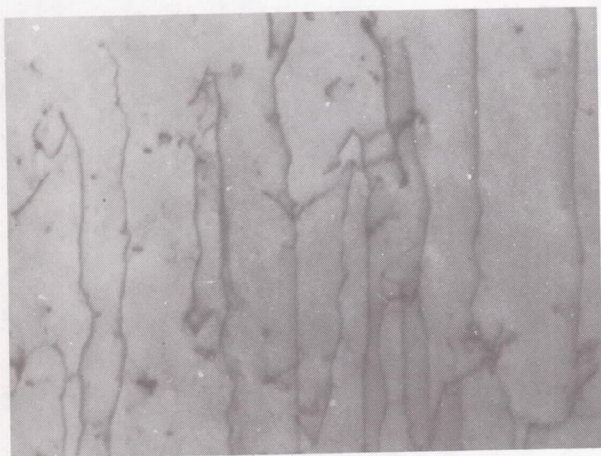
Deformation to 5.0 percent strain results in complex dislocation substructures, as shown in figure 6. Dislocation tangling is observed in single crystal tungsten and W-1Re (figs. 6(a) and (b)). Formation of edge dipoles behind screw dislocations characterizes the W-3Re alloy. Single crystal W-Ta alloys are characterized by long screw dislocations with some debris formation occurring.

Temperature dependence of dislocation substructures after 2.0 percent deformation is illustrated in figures 5, 7, and 8 at temperatures of 300, 150, and 590 K, respectively. Specimens deformed at 150 and 300 K (0.04 and $0.08 T_m$) are characterized by long screw dislocations lying parallel to the primary [111] slip direction. In general, dislocations were noted to be aligned more strongly in the [111] direction at 150 K than at 300 K, which may be related to the higher applied stress at the lower temperature. In contrast to the fairly small jogs on relatively straight screw dislocations in unalloyed tungsten, much larger jogs and a higher radius of curvature of the dislocation lines were observed in the W-Re alloy crystals. In addition, at 150 K predominately edge dipoles are formed and mixed dislocations are present in the W-Re alloys. Tantalum additions did not alter the dislocation substructure to the same degree as rhenium additions; however, formation of predominately edge dipoles seemed to be more common in W-Ta alloys than in unalloyed tungsten.

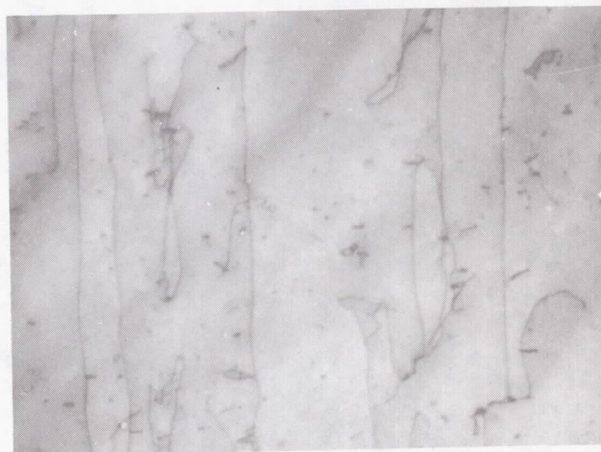
Tungsten and tungsten alloy crystals tested at 590 K or $0.16 T_m$ were characterized primarily by dislocations with long edge components, as shown in figure 8. Edge-type dipoles with a length to width ratio of 10 are common in the W-Re alloy crystals at 590 K compared with ratios of 4 and 2 at test temperatures of 300 and 150 K, respectively. In contrast, the few dipoles observed in tungsten at 300 K and more abundantly at 590 K had length to width ratios of 2 and 3, respectively. A very low density of straight screw dislocations was observed in single crystal tungsten. In the W-Re crystals, alignment parallel to the primary [111] slip direction is essentially nonexistent. Dislocations are either of edge character or long, mixed dislocations. Braids of dislocations consisting primarily of edge dislocations characterized the W-1Ta alloy. The braids lie parallel to the [010] direction and are spaced approximately 2 micrometers apart. The W-3Ta crystal was characterized primarily by edge dipoles with length to width ratios of 5.



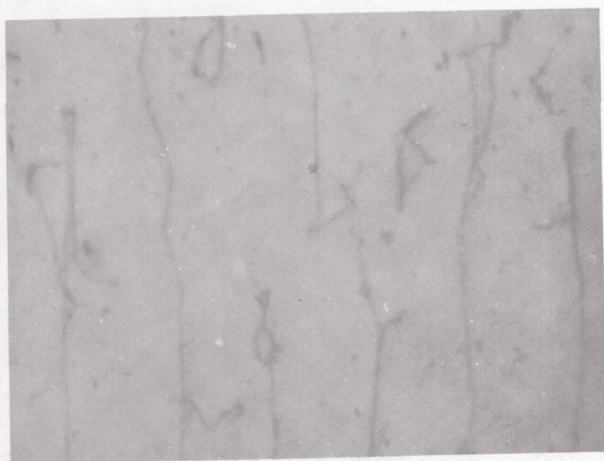
(a) Unalloyed tungsten.



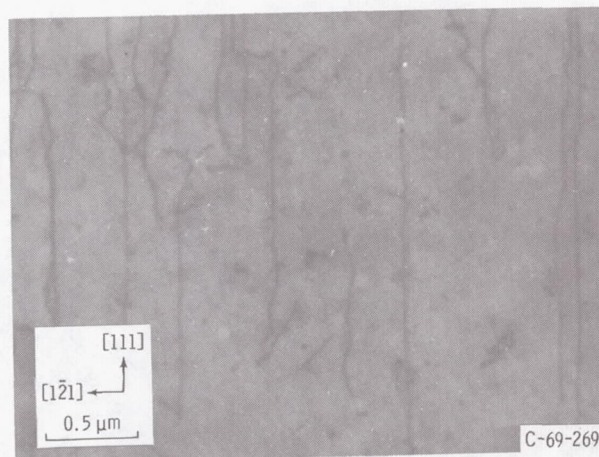
(b) W - 1 percent Re.



(c) W - 3 percent Re.

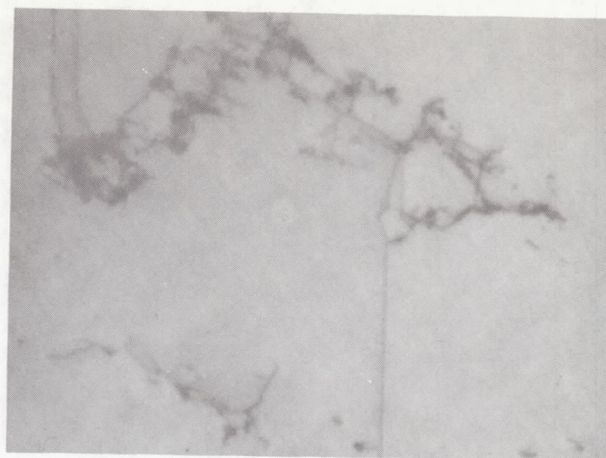


(d) W - 1 percent Ta.

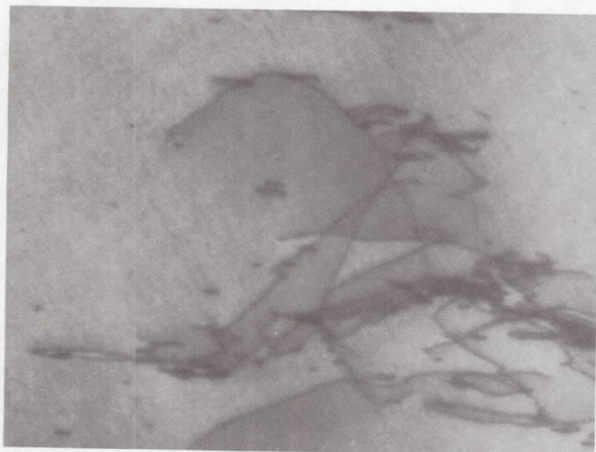


(e) W - 3 percent Ta.

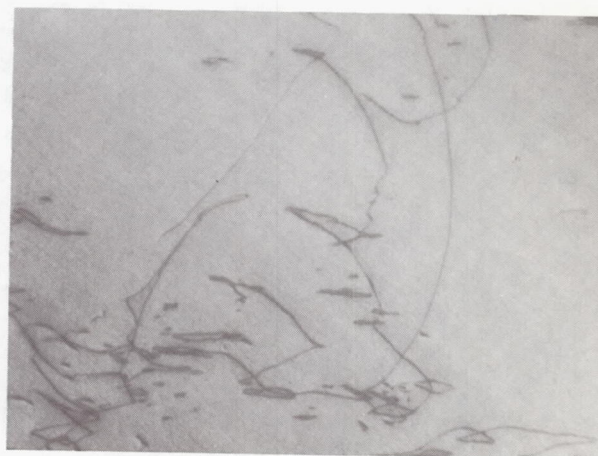
Figure 7. - Dislocation structures after 2.0 percent strain at 150 K.



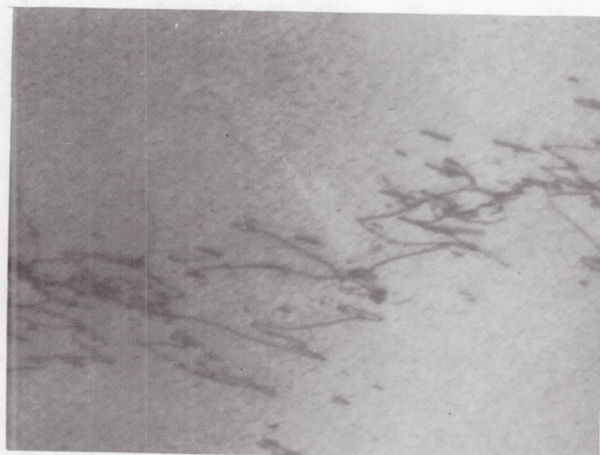
(a) Unalloyed tungsten.



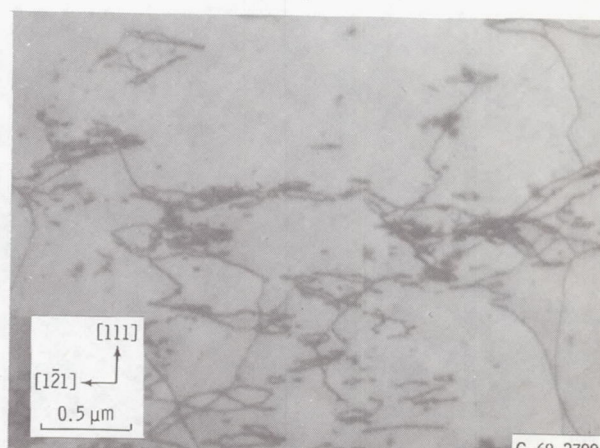
(b) W - 1 percent Re.



(c) W - 3 percent Re.



(d) W - 1 percent Ta.



(e) W - 3 percent Ta.

Figure 8. - Dislocation structures after 2.0 percent strain at 590 K.

C-69-2700

The effect of solute content on dislocation density of single crystal tungsten is shown in figure 9 for a constant strain of 2.0 percent at the three test temperatures. It should be noted that dislocation density varies linearly with solute content over the temperature range 150 to 590 K. Also, rhenium additions increase dislocation density slightly more than equivalent tantalum additions at each temperature.

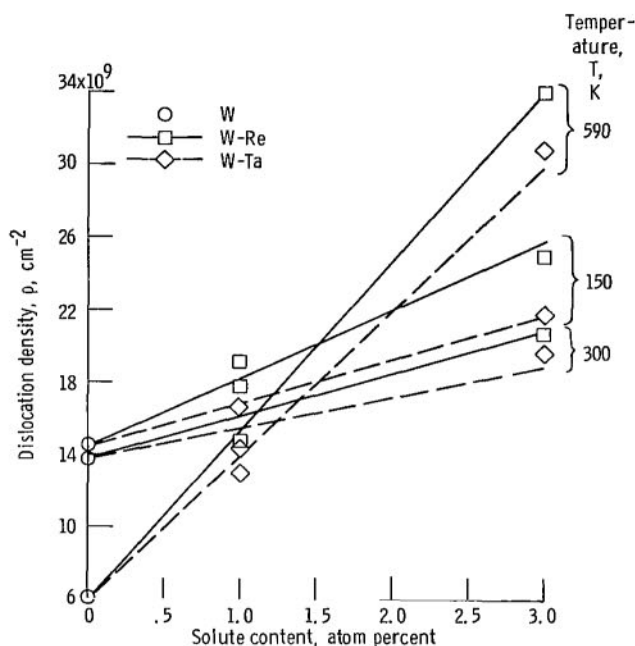
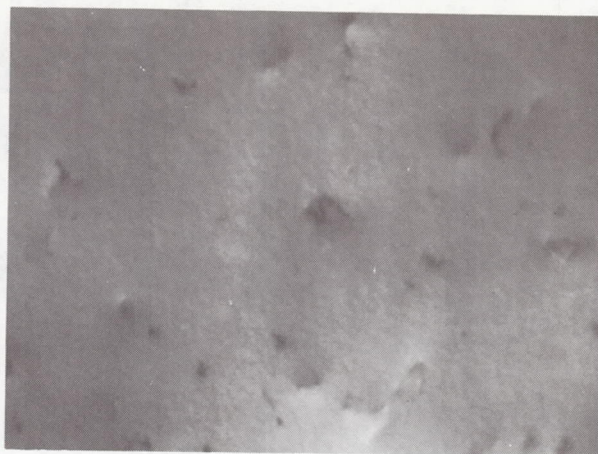


Figure 9. - Effect of solute content on dislocation density of W after 2.0 percent strain.

Foils from each specimen were examined using different operating reflections in order to verify Burgers vectors for the long screw dislocations and the edge dipoles observed in the foils. From the theory of electron diffraction contrast (Howie, ref. 18), if \bar{g} is the reciprocal lattice vector of the reflecting plane and \bar{b} is the Burgers vector, the contrast intensity for the dislocation is zero when $\bar{g} \cdot \bar{b} = 0$. If $\pm a/2 [111]$ is taken as the primary Burgers vector, all dislocations belonging to the primary slip system $(\bar{1}01) [111]$ will have zero contrast intensity using an operating reflection such as $\bar{1}\bar{2}1$ (i.e., $\bar{g} \cdot \bar{b} = 0$). Specimens deformed at 150 K to 2.0 percent strain were examined using the $\bar{1}\bar{2}1$ reflection. For W-Re alloys, a second weak reflection also operated. Figure 10 illustrates the zero contrast intensity for the primary Burgers vector $\pm a/2 [111]$. This figure should be compared with figure 7 where the dislocations (in different areas of the same foils but having essentially the same structure) are in strong contrast using different operating reflections. It should be noted for the W-Re alloys that dislocations



(a) Unalloyed tungsten.



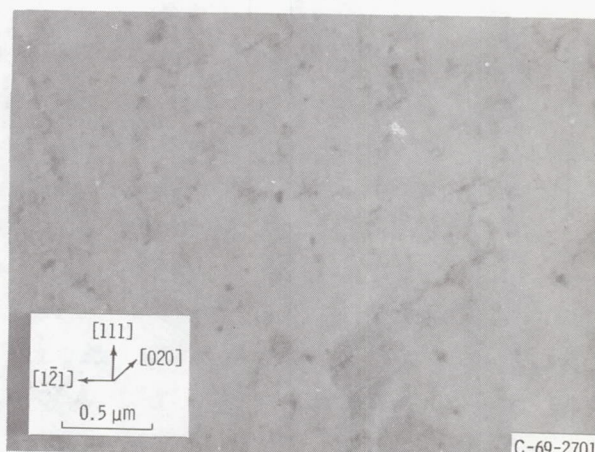
(b) W - 1 percent Re.



(c) W - 3 percent Re.



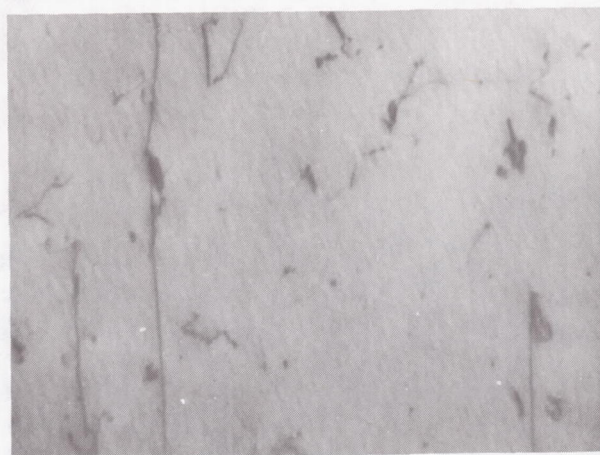
(d) W - 1 percent Ta.



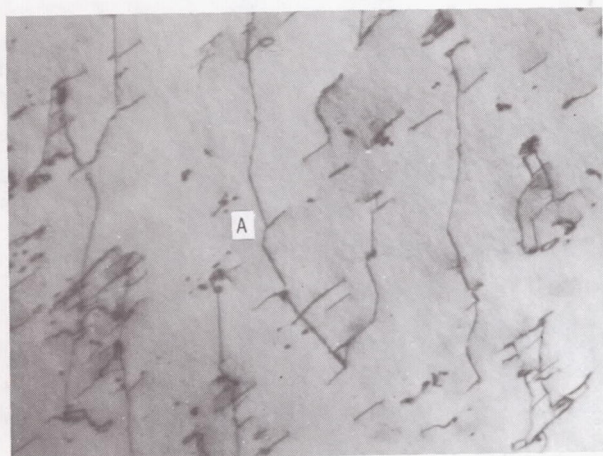
(e) W - 3 percent Ta.

C-69-2701

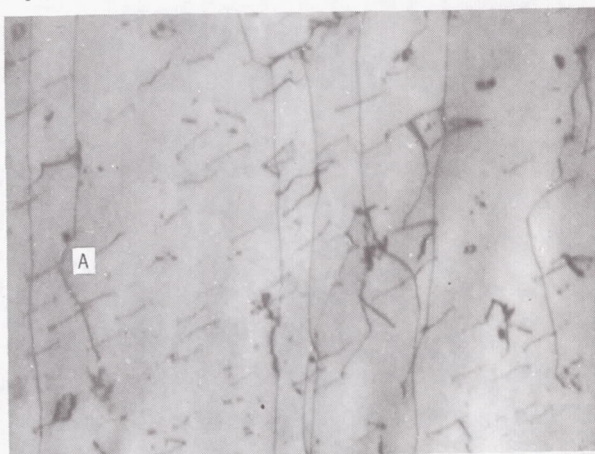
Figure 10. - Dislocation structures with $g \cdot b = 0$. Strain is 2.0 percent at 150 K.



(a) Unalloyed tungsten.



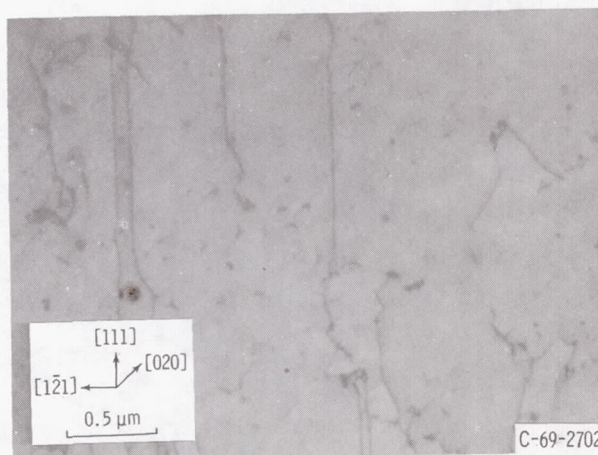
(b) W - 1 percent Re.



(c) W - 3 percent Re.



(d) W - 1 percent Ta.



(e) W - 3 percent Ta.

Figure 11. - Dislocation structures with $g = 0\bar{2}0$. Strain is 2.0 percent at 150 K.

C-69-2702

whose projections lie parallel to the $[020]$ direction have moderate contrast intensity in figures 10(b) and (c). By using the $0\bar{2}0$ reflection for the same area of the foils, these dislocations were brought into much stronger contrast intensity, as shown in figures 11(b) and (c). Dislocations of this type are not observed in unalloyed tungsten or W-1Ta using the same operating reflection (figs. 11(a) and (d)), however, a few are observed in the W-3Ta alloy (fig. 11(e)). An analysis of the directions of these secondary dislocations using the previous extinction experiments indicated that they are consistent with $(1\bar{1}2)$ $[\bar{1}11]$ slip. Since $(1\bar{1}2)$ $[\bar{1}11]$ slip was not observed in unalloyed tungsten, this suggests that rhenium and tantalum additions change the ratio of critical resolved shear stress on $(\bar{1}01)$ to that on $(1\bar{1}2)$. Based on the Schmid factors it is estimated that this change is approximately 14 percent.

DISCUSSION

Temperature Dependence of Dislocation Substructures in Tungsten

A comparison of the dislocation substructures observed in single crystal tungsten will be made with similar observations reported elsewhere for the other refractory metals, niobium, tantalum, and molybdenum, at equivalent homologous temperatures. At an equivalent amount of strain, marked differences in dislocation substructures are observed in this study at different test temperatures in single crystal tungsten. At 150 and 300 K (0.04 and $0.08 T_m$), long screw dislocations lying parallel to the primary $[111]$ slip direction characterize the structure while at 590 K or $0.16 T_m$ the structure is characterized predominately by edge dislocations with a notable low density of screw dislocations.

Table II summarizes the dislocation substructures observed in tungsten and the other refractory metals along with the type of hardening at each temperature, as determined from the stress-strain curves. It should be noted that, when compared on the basis of homologous temperature, dislocation structures observed in tungsten are similar to those observed in the other refractory metals. At homologous temperatures greater than $0.1 T_m$, the dislocation structures in the refractory metals are characterized predominantly by edge dislocations. At homologous temperatures less than $0.1 T_m$, screw dislocations characterize the structures of the refractory metals. It should also be noted in table II that both edge and screw dislocations have been observed during stage II hardening. The type of dislocation structure formed appears to depend on the homologous temperature rather than on type of hardening.

The presence of edge or screw dislocations apparently can be attributed to the difference in their mobilities in body-centered cubic metals and solid solutions due to the difference in the Peierls stress of edge (low Peierls stress) and screw (high Peierls

TABLE II. - COMPARISON OF DISLOCATION STRUCTURES

OBSERVED IN REFRACTORY METALS

Refractory metal	Deformation temperature, K	Homologous temperature	Dislocation structure	Type of hardening	Reference
Nb	295	0.11	Edge	Stage I, II	5, 6
	158	.06	Screw	Stage II	6
Ta	463	0.14	Edge	Stage II	8
	273	.08	Screw	Parabolic	8
Mo	578	0.20	Edge	Linear	11
	373	.13	Edge	Parabolic	9
	4.2 to 300	0.0015 to 0.1	Screw	Parabolic	10
W	590	0.16	Edge	Linear	This report
	150 to 300	0.04 to 0.08	Screw	Parabolic	This report

stress) dislocations as discussed by Arsenault and Lawley (ref. 8). At small effective stresses, that is, $T > 0.1 T_m$, the internal stress is a large component of the applied stress and hence a major barrier to dislocation motion. Therefore edge components may be stopped at positions where the internal stress is only slightly higher than the average applied stress. However, at a high applied stress, that is, $T < 0.1 T_m$ the edge component will not be held up at these positions of slightly high stress fields and will move out of the lattice leaving behind long screw dislocations.

It is pertinent to note that temperatures above the ductile-brittle transition temperature of unalloyed polycrystalline tungsten tested in tension at approximately the same strain rate used in this study coincide with the temperature where edge dislocations predominate the substructure in single crystal tungsten. Both rhenium and tantalum additions promote formation of edge dipoles at lower temperatures and also result in a reduction of the ductile-brittle transition temperature, thus suggesting that screw dislocation mobility is a critical factor in determining the ductility of body-centered metals. Niobium tested at $0.06 T_m$ (ref. 6), although characterized by screw dislocations, contained a large amount of debris or edge dipoles and of course is ductile at this temperature.

Implications of the Dilute Rhenium Ductilizing Effect

Additions of rhenium to tungsten in amounts less than approximately 5.0 percent have been shown by Klopp et al. (ref. 12) to lower the ductile-brittle transition temperature of recrystallized electron beam melted tungsten. This is illustrated in figure 12

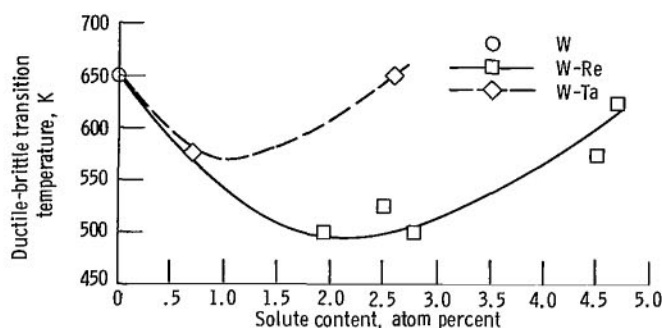


Figure 12. - Effect of solute content on ductile-brittle transition temperature of polycrystalline electron beam melted W (ref. 17 and unpublished data obtained by Witzke of Lewis).

along with unpublished data on W-Ta alloys obtained by W. R. Witzke of Lewis Research Center. It should be noted that dilute tantalum additions also slightly lower the ductile-brittle transition temperature.

The most significant effect of rhenium additions to tungsten observed in this investigation on single crystals is the formation of edge dipoles in the wake of screw dislocations at temperatures of 150 and 300 K, 0.04 and 0.08 T_m , respectively. This evidence along with larger jogs formed on screw dislocations and a higher dislocation density in W-Re crystals compared with unalloyed tungsten suggests that the primary effect of rhenium additions is to increase dislocation mobility. Adding rhenium to tungsten results in the formation of edge dipoles with length to width ratios substantially greater than 1, suggesting that screw dislocation mobility has been increased to a greater degree than edge dislocation mobility. The mechanism by which rhenium additions promote increased screw dislocation mobility, which in turn leads to increased ductility or solution softening in tungsten is considered to be lowering the Peierls-Nabarro force or inherent lattice resistance to dislocation motion. Based on evidence of large jogs on screw dislocations and cell formation in polycrystalline W-3Re and W-9Re alloys after only 2 percent strain at room temperature, a similar conclusion was arrived at in reference 4. Gilbert et al. (ref. 19) also arrived at a similar conclusion with regard to low-temperature hardness results on chromium-rhenium alloys. Mitchell and Raffo (ref. 20) have suggested that broadening of the dislocation core in the vicinity of a solute atom may account for the reduction in the Peierls-Nabarro force. It would then be expected that other solute atoms would have similar effects and it is observed that tantalum additions in tungsten also lower the ductile-brittle transition temperature.

Offsetting this ductilizing effect is the normally observed solution hardening effect caused by distortion of the lattice in the vicinity of solute atoms resulting in embrittlement. The two competing processes are responsible for the minimum in the curve of flow stress as a function of concentration of solute shown in figure 3. This offsetting

effect would be expected to be stronger with tantalum additions than with rhenium additions based on atomic size differences. Observations of foils in this study suggest that tantalum additions are not as effective as rhenium additions in increasing dislocation mobility as evidenced by fewer edge dipoles in W-Ta alloys and an overall lower dislocation density compared with W-Re alloys.

Promotion of $(1\bar{1}2)$ $[\bar{1}11]$ slip may also be considered as contributing to increased dislocation mobility in that it provides slip on a second plane. However, offsetting this is the subsequent increase in flow stress as the solute content is increased from 1 to 3 percent (fig. 3), which is attributed to an interaction of dislocations on the $(\bar{1}01)$ plane with those on the $(1\bar{1}2)$ planes as noted at A in figures 11(b) and (c).

SUMMARY OF RESULTS

The observations from this study of the effects of strain, temperature, and alloying on the dislocation substructures in single crystal tungsten can be summarized as follows:

1. Dilute rhenium additions in single crystal tungsten increase dislocation mobility as evidenced by formation of edge dipoles and an increase in dislocation density. At the lowest temperatures investigated, 150 K, rhenium additions produced dislocations consistent with $(1\bar{1}2)$ $[\bar{1}11]$ slip in addition to slip on the primary $(\bar{1}01)$ slip plane.

2. Tantalum additions in tungsten also increase dislocation density, but are not as effective as rhenium in promoting formation of edge dipoles or dislocations consistent with $(1\bar{1}2)$ $[\bar{1}11]$ slip.

3. Dislocation structures observed in tungsten at $T > 0.1 T_m$ (fraction of absolute melting temperature) are similar to structures observed in other refractory metals at an equivalent homologous temperature. Clusters of predominately edge dipoles characterize the structure with a notable low density of $[111]$ screw dislocations in the $(\bar{1}01)$ slip plane.

4. Dislocation structures observed in tungsten at $T < 0.1 T_m$ are also similar to structures observed in the other refractory metals at equivalent homologous temperatures. Long screw dislocations lying parallel to the primary slip direction characterize the dislocation structure.

It is concluded that the increase in ductility of polycrystalline tungsten containing dilute rhenium and tantalum additions at temperatures below $0.1 T_m$ is associated with an increase in screw dislocation mobility which is indicated by formation of edge dipoles at temperatures as low as $0.04 T_m$.

Lewis Research Center,
National Aeronautics and Space Administration,
Cleveland, Ohio, August 6, 1969,
129-03.

REFERENCES

1. Harris, B.: Solution Hardening in Niobium. *Phys. Status Solidi*, vol. 18, 1966, pp. 715-730.
2. Barbee, Troy W., Jr.; and Huggins, Robert A.: Dislocation Structures in Deformed and Recovered Tantalum. *J. Less-Common Metals*, vol. 8, no. 5, May 1965, pp. 306-319.
3. Gilbert, A.; Wilcox, B. A.; and Hahn, G. T.: The Effect of Strain Rate on Dislocation Multiplication in Polycrystalline Molybdenum. *Phil. Mag.*, vol. 12, no. 117, Sept. 1965, pp. 649-653.
4. Stephens, Joseph R.: Dislocation Structures in Slightly Strained Tungsten, Tungsten-Rhenium, and Tungsten-Tantalum Alloys. *Trans. AIME*, vol. 242, no. 4, Apr. 1968, pp. 634-640.
5. Foxall, R. A.; Duesbery, M. S.; and Hirsch, P. B.: The Deformation of Niobium Single Crystals. *Can. J. Phys.*, vol. 45, no. 2, pt. 2, Feb. 1967, pp. 607-629.
6. Bowen, D. K.; Christian, J. W.; and Taylor, G.: Deformation Properties of Niobium Single Crystals. *Can. J. Phys.*, vol. 45, no. 2, pt. 3, Feb. 1967, pp. 903-938.
7. Spitzig, W. A.; and Mitchell, T. E.: Dislocation Arrangements in Tantalum Single Crystals Deformed in Tension at 373° K. *Acta Met.*, vol. 14, Oct. 1966, pp. 1311-1323.
8. Arsenault, R. J.; and Lawley, A.: Work Hardening and Dislocation Structure in Ta and Ta-Base Alloys. *Phil. Mag.*, vol. 15, no. 135, Mar. 1967, pp. 549-565.
9. Loesch, H. W., Jr.; and Brotzen, F. R.: Observation of Dislocations in Deformed Molybdenum Crystals. *J. Less-Common Metals*, vol. 13, no. 6, Dec. 1967, pp. 565-578.
10. Lawley, A.; and Gaigher, H. L.: Deformation Structures in Zone-Melted Molybdenum. *Phil. Mag.*, vol. 10, no. 103, July 1964, pp. 15-33.
11. Lawley, A.: Deformation Structures in Zone-Melted Molybdenum Above Room Temperature. *Refractory Metals and Alloys IV: Research and Development*. Vol. 1. R. I. Jaffee, G. M. Ault, J. Maltz, and M. Semchyshen, eds., Gordon and Breach Science Publ., 1968, pp. 141-160.
12. Klopp, William D.; Witzke, Walter R.; and Raffo, Peter L.: Mechanical Properties of Dilute Tungsten-Rhenium Alloys. *NASA TN D-3483*, 1966.

13. Schoone, R. D.; and Fischione, E. A.: Automatic Unit for Thinning Transmission Electron Microscopy Specimens of Metals. *Rev. Sci. Instr.*, vol. 37, no. 10, Oct. 1966, pp. 1351-1353.
14. Hirsch, P. B.; Howie, A.; Nicholson, R. B.; Pashley, D. W.; and Whelan, M. J.: *Electron Microscopy of Thin Crystals*. Butterworth & Co., 1965.
15. Garlick, R. G.; and Probst, H. B.: Investigation of Room-Temperature Slip in Zone-Melted Tungsten Single Crystals. *Trans. AIME*, vol. 230, no. 5, Aug. 1964, pp. 1120-1125.
16. Garfinkle, M.: Room-Temperature Tensile Behavior of $\langle 100 \rangle$ Oriented Tungsten Single Crystals with Rhenium in Dilute Solid Solution. NASA TN D-3190, 1966.
17. Raffo, P. L.: Yielding and Fracture in Tungsten and Tungsten-Rhenium Alloys. *J. Less-Common Metals*, vol. 17, no. 2, Feb. 1969, pp. 133-149.
18. Howie, A.: Interpretation of Transmission Electron Microscope Images of Dislocations and Stacking Faults. *Direct Observation of Imperfections in Crystals*. J. B. Newkirk and J. H. Wernick, eds., Interscience Publ., 1962, pp. 269-282.
19. Gilbert, A.; Klein, M. J.; and Edington, J. W.: Investigation of Mechanical Properties of Chromium, Chromium-Rhenium, and Derived Alloys. Battelle Memorial Inst. (NASA CR-81225), Aug. 31, 1966.
20. Mitchell, T. E.; and Raffo, P. L.: Mechanical Properties of Some Tantalum Alloys. *Can. J. Phys.*, vol. 45, no. 2, pt. 3, Feb. 1967, pp. 1047-1062.

FIRST CLASS MAIL



POSTAGE AND FEES PAID
NATIONAL AERONAUTICS &
SPACE ADMINISTRATION

NOV 11 1968 65286 00903
MAIL ROOM
NATIONAL AERONAUTICS & SPACE ADMINISTRATION

POSTMASTER: If Undeliverable (Section 15
Postal Manual) Do Not Return

"The aeronautical and space activities of the United States shall be conducted so as to contribute . . . to the expansion of human knowledge of phenomena in the atmosphere and space. The Administration shall provide for the widest practicable and appropriate dissemination of information concerning its activities and the results thereof."

— NATIONAL AERONAUTICS AND SPACE ACT OF 1958

NASA SCIENTIFIC AND TECHNICAL PUBLICATIONS

TECHNICAL REPORTS: Scientific and technical information considered important, complete, and a lasting contribution to existing knowledge.

TECHNICAL NOTES: Information less broad in scope but nevertheless of importance as a contribution to existing knowledge.

TECHNICAL MEMORANDUMS: Information receiving limited distribution because of preliminary data, security classification, or other reasons.

CONTRACTOR REPORTS: Scientific and technical information generated under a NASA contract or grant and considered an important contribution to existing knowledge.

TECHNICAL TRANSLATIONS: Information published in a foreign language considered to merit NASA distribution in English.

SPECIAL PUBLICATIONS: Information derived from or of value to NASA activities. Publications include conference proceedings, monographs, data compilations, handbooks, sourcebooks, and special bibliographies.

TECHNOLOGY UTILIZATION PUBLICATIONS: Information on technology used by NASA that may be of particular interest in commercial and other non-aerospace applications. Publications include Tech Briefs, Technology Utilization Reports and Notes, and Technology Surveys.

Details on the availability of these publications may be obtained from:

SCIENTIFIC AND TECHNICAL INFORMATION DIVISION
NATIONAL AERONAUTICS AND SPACE ADMINISTRATION
Washington, D.C. 20546